Journal of Simulation and Analysis of Novel Technologies in Mechanical Engineering
16 (1) (2024) 0005~0021
DOI 10.71939/jsme.2024.1092091

Research article

Conceptual design of the inlet flow preheat system for nozzle test equipment of a turbine engine

Behrooz Shahriari*, Hamid Farrokhfal, Mohammad Reza Nazari

Faculty of Mechanics, Malek Ashtar University of Technology, Iran

*shahriari@mut-es.ac.ir

(Manuscript Received --- 01 Oct. 2023; Revised --- 21 May 2024; Accepted --- 16 June 2024)

Abstract

To ensure the correct design and proper operation of turbine engine components, various types of ground tests must be performed, which requires the simulation of the input flow to these components. To test hot components such as nozzles, it is necessary to create a hot flow, which is done by the preheat system of the inlet flow. For the ground test of the nozzle of a turbofan engine that has an afterburner in addition to the combustion chamber, the preheat system must be able to supply air in two modes, dry mode and reheat mode. In this paper a combustion chamber with an afterburner is used to provide hot air to the nozzle. In the first step, using experimental and analytical relations, the combustion chamber is designed. The presented algorithm has the ability to calculate the diameter and reference surface of the combustion chamber, components of the combustion chamber and thermodynamic parameters. Then the obtained results are compared with the data of a similar annular combustion chamber. The comparison indicates the acceptable convergence of the design results with the experimental results. Finally, the output flow of the combustion chamber is considered as the input of the afterburner, and the temperature of the combustion flow is increased by the afterburner to the desired temperature. In addition to the ability to design a V-gutter flame keeper, the afterburner design algorithm also calculates the thermodynamic characteristics of the afterburner output stream, considering the requirements of flame stability.

Keywords: Turbofan engine nozzle, Nozzle ground test, Hot flow simulation, Combustion chamber design, Afterburner design.

1- Introduction

The testing of the main components of the turbine engines as well as the integrated testing of the entire propulsion system includes hours of ground and flight testing. The ground test of the main components, including the compressor, combustion chamber, turbine, afterburner, and nozzle, requires a special test room for each of these components. Compressed air supply facilities and the preheat section of the flow are needed to simulate the cold and hot inlet flow. Since the nozzle of the turbofan engine has an afterburner in addition to the main combustion chamber, the preheat system must have the ability to create the inlet temperature conditions for the nozzle in two modes, afterburner on and afterburner off. In fact, the preheat system used in the nozzle test room has

two sections, the combustion chamber and the afterburner, which operate depending on the need. Therefore, the design of this ground preheat system has its own complexities, and the method of designing the main components of the nozzle and afterburner in air turbine engines can be used in this direction. However, due to the fact that this preheat system is on the ground, some air requirements such as minimum weight can be ignored or a cooling method other than air can be used to increase the cooling efficiency. The design of gas turbine combustion chamber and combustion analysis has been a serious challenge for researchers due to the existing complexities such as turbulence, chemical kinetics, thermal radiation and the production of pollutants. Large manufacturing companies use expensive programs to upgrade and improve the combustion chamber of turbine engines, and most of these methods have achieved their desired combustion chamber after initial designs with methods based on trial and error [1]. Also, these companies have obtained their own rules by using laboratory tests and experience, which help in product development and improvement programs. These design rules provide solutions to achieve the desired chamber geometry given the inlet conditions. If a combustion chamber designer does not have access to these solutions, it is necessary to obtain his own design method using available sources such as articles and experiments. However, a significant number of empirical, semi-empirical, and analytical relationships are available that minimize the need for costly experimental tests. In addition, in the combustion chamber design process, the use of advanced computational methods and accurate modeling of combustion flow behavior can reduce the number of laboratory tests and make the design process shorter and less costly. Combustion chamber designers have always sought to design a combustion chamber that, in addition to high efficiency and low pressure drop, has an optimal outlet temperature and a long service life. Mattingly [2] and Lefebvre [3] presented a set of empirical, semi-empirical relationships and analytical models that are used in the design of conventional combustion chambers of turbine engines. They have also provided information and solutions regarding new generations of modern enclosures. Charest presented relationships for the preliminary design of a can-type combustor. The presented method was based on component modeling and phenomena such as droplet evaporation, heat transfer and jet mixing were modeled in it. He compared and evaluated the results of his method in which he used empirical and semi-empirical relations with the computational fluid dynamics solution of a combustion chamber [4]. In another study, Stuttsford and Rubini modeled flow and heat transfer using a network method. This method divides the chamber into several separate and internally connected control volumes. Then the continuity, momentum and energy equations are discretized for different control volumes and by solving the equations, internal flow and temperature variables are obtained at different points [5]. Khandelwal designed the combustion chamber with the approach of reducing pollutants and studied the effect of different geometrical parameters on the performance of the combustion chamber composite diffuser [6]. In the process of designing a new generation of Rolls-Royce combustion chambers,

Wankhede used a combined method using CFD and experimental relationships [7]. Jai-Houng Leu designed and simulated a combustion chamber used in a gas turbine, the fuel used is of low heating value type, and the source of this fuel is the gaseous cation produced in the combustion of waste plastic. He also evaluated the performance of the designed chamber according to previous works and one-dimensional flow characteristics [8]. Yize Liu et al. developed a general framework for the preliminary design of air turbine combustion chambers. Design elements were a combination of flow distribution, combustion chamber size, heat transfer and cooling, pollutant levels, and other performance parameters. The presented numerical method was based on experimental and semi-experimental methods and the accuracy of the design was checked using previous works [9]. The review of the research conducted in the field of combustion chamber and afterburner of turbine engines show that so far no research has been presented on the design and analysis of the two-stage engine preheat system. In the present study, a combustion chamber with an afterburner (without the use of a turbine) was used in an innovative way to supply air to the nozzle test system. At first, according to the semi-experimental and analytical relations, the geometric and thermodynamic characteristics of the combustion chamber were determined, and then the obtained results were validated with the data of a similar combustion chamber. Finally, the temperature of the exit stream from the combustion chamber has been increased to the desired value by an afterburner designed by reverse engineering method and empirical relationships.

2- Combustion chamber design algorithm and method

In this section, the combustion chamber is done at the conceptual design level. In the first step, the diameter of the liner and the reference surface of the combustion chamber are determined. Then, according to the inputs of the problem and the relationships extracted from the authoritative sources, the two-dimensional geometry of the combustion chamber is produced and by using the relations of the combustion flows, the characteristics of the output flow of the combustion chamber are predicted. Fig. 1 shows the combustion chamber design algorithm.

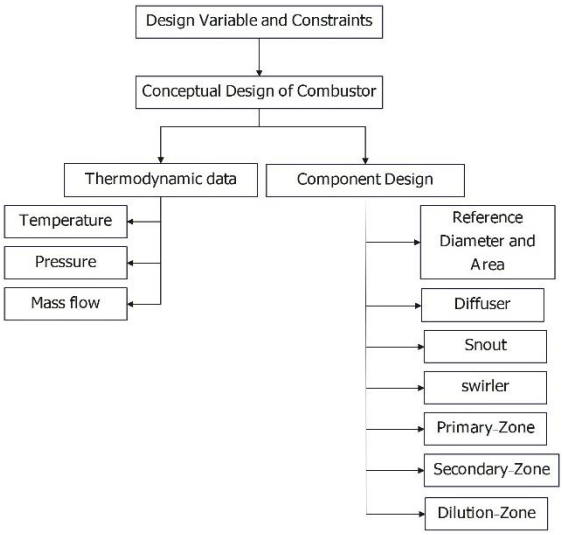

Fig. 1 Combustion chamber design algorithm

2-1- Reference diameter and liner diameter

The first step in designing the combustion chamber is to determine the reference diameter (D_{ref}). The reference diameter is the same as the diameter of the combustion chamber shell, and in most references, the reference diameter is calculated by considering chemical considerations or pressure drop. After determining the reference diameter, the diameter of the liner (D_{ft}) is calculated. Fig. 2 shows the

reference diameter and liner diameter of conventional
combustion chambers. Estimation of the reference diameter can be done based on different methods. Various algorithms and methods have been presented in different references to estimate the reference diameter and liner diameter and how these two sections are related. In this work, four different methods are used to obtain these values as follows.

One of the reference diameter estimation methods is the aerodynamic requirements method, which is based on the pressure drop ratio and pressure factor.

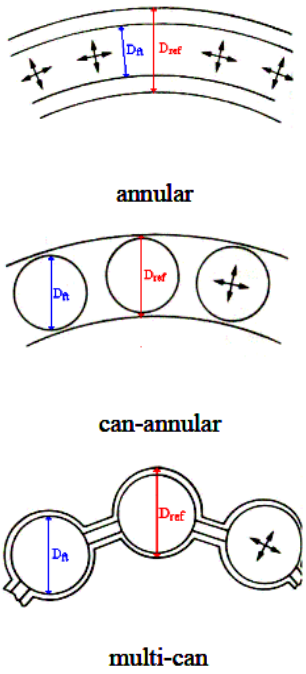

Fig. 2 Reference diameter and liner diameter in combustion chamber types

In general, if the combustion chamber is large enough to accommodate a certain pressure drop, it will be large enough to accommodate the chemical reactions. Sometimes, depending on the conditions, the diameter obtained from the reaction rate equations may be greater than the diameter obtained from the aerodynamic method, in which case the combustion engineer is responsible for determining the correct method [10]. In this method, the reference level is calculated from equation (1).

$$A_{ref} = \left(143.5 \left(\frac{\dot{m}_3 T_3^{0.5}}{P_3} \right)^2 \left(\frac{\frac{\Delta P_{3-4}}{q_{ref}}}{\frac{\Delta P_{3-4}}{p_3}} \right) \right)^{0.5} \quad (1)$$

where $\left(\frac{\Delta P_{3-4}}{P_3}\right)$ is called the total pressure drop and expresses the ratio of the total pressure drop to the total inlet pressure at the time of ignition. This parameter is usually expressed as a percentage (usually between 4 and 8) and depends on the operational conditions of the combustion chamber. The term $\left(\frac{\Delta P_{3-4}}{q_{ref}}\right)$ is called the pressure factor and it expresses the ratio of the total pressure to the reference dynamic pressure at the time of ignition. This parameter is very important for combustion engineers, because it represents the resistance of the current applied between the compressor outlet and the turbine inlet. From aerodynamic point of view, this parameter can be considered equivalent to the Drag coefficient, which is one of the constant characteristics of the combustion chamber (it does not depend on the operating conditions). Also, this parameter indicates the total pressure drop in the diffuser and throughout the liner, which is shown as Eq. (2) [3].

$$\frac{\Delta P_{3-4}}{q_{ref}} = \frac{\Delta P_{diff}}{q_{ref}} + \frac{\Delta P_L}{q_{ref}} \quad (2)$$

In addition to aerodynamic requirements, the combustion chamber must be designed in such a way that it is possible to carry out combustion processes in it. The method of combustion requirements, taking into account the geometrical conditions

necessary for combustion, determines the reference diameter necessary to carry out the combustion reaction in different working conditions. Lefebvre stated that for any specific ratio of fuel to air, the combustion efficiency (η) is a function of the parameter θ, which is equal to Eq. (4).

$$\eta_c = \eta_\theta = f(\theta) \tag{3}$$

$$\theta = \frac{P_3^{1.75} A_{ref} D_{ref}^{0.75} \exp(\frac{T_3}{b})}{\dot{m}_3} \tag{4}$$

In the above equation, parameter b is the temperature correction and its value can be considered as 300 degrees Kelvin on average. In order to calculate more accurately, the temperature correction parameter as a function of equivalence in the initial area of the combustion chamber can be expressed as equation (5).[2]

$$\begin{aligned} b &= 245(1.39 + ln\varphi_{pz}) \quad for\ 0.6 < \varphi_{pz} < 1.0 \\ b &= 170(2.0 - ln\varphi_{pz}) \quad for\ 1.0 < \varphi_{pz} < 1.4 \end{aligned} \tag{5}$$

where b is in Kelvin and φ_{pz} is the equivalence ratio of fuel and air mixing in the initial area of the combustion chamber. Another method that calculates the reference diameter by considering the combustion requirements and flame stability is called the combustion loading method, in which the volume of the combustion chamber is calculated with loading parameters. The study [11] presented Eq. (6) for the loading parameter:

$$Loading = \frac{\dot{m}_3}{V\ P_3^{1.8} 10^{(0.00145*(T_3-400))}} \tag{6}$$

where, $\dot{m}_3$ is the mass flow rate in Kg/s, V is the combustion chamber volume in m^3, P_3 is the inlet pressure in atm and T_3 is the inlet temperature in Kelvin. The maximum loading parameter value occurs for the highest flight altitude, the lowest flight Mach Number and the coldest weather conditions.

In this situation, in order to create a sufficient margin of confidence to prevent flame extinction and achieve acceptable efficiency, this parameter is considered less than 50. Also, for the conditions of the sea level and the highest thrust, the loading parameter is recommended to be less than 10 and preferably less than 5. The combustion intensity parameter is a measure of the heat released per unit volume of the combustion chamber and is defined as Eq. (7)

$$Intensty = \frac{\dot{m}_{fuel}\, \eta_c\, LHV}{V\ P_3} \tag{7}$$

where LHV is the minimum thermal energy of the fuel in terms of (KJ/Kg) and η_c is the combustion efficiency in the combustion chamber. From another point of view, the loading parameter is also a measure of the difficulty of combustion, so it is desirable to have a low value. For design conditions (operating conditions at sea level and maximum thrust), the combustion intensity should be less than 60. This value is achievable for industrial engines, but it can be challenging for aero engines. Also, in the industrial gas turbine, this value may be considered lower due to the larger available combustion space and due to the possibility of using a converter and the need for less heat. The volume of the combustion chamber should be such as to ensure that the loading parameter corresponds to the intensity of combustion. The volume of the chamber can be calculated from Eq. (8):

$$V = \frac{\dot{m}_a}{Loading \times {P_3}^{1.8} 10^{(0.00145 \times T_{31} - 400)}} \tag{8}$$

Where γ is the ratio of thermal coefficient at constant pressure to constant volume and $\frac{P}{PS}$ is the ratio of total pressure to static pressure. Having the cross section of the liner and the volume of the combustion chamber, the length of the chamber is obtained from Eq. (9):

$$L = \frac{V}{A_{ft}} \tag{9}$$

Now the residence time can be checked with Eq. (10). The residence time is the time it takes for an air molecule to pass through the combustion chamber, which must be more than 3 ms in order to fully mix fuel and air and have a complete combustion. It is important to note that by increasing the mass flow rate entering a combustion chamber with a certain geometry, the flow Mach Number increases and as a result, the residence time decreases.

$$Residence\ Time = \frac{L_{combustor}}{M\sqrt{\gamma RT}} \tag{10}$$

Different sources have provided several methods to estimate the area of the combustion zone A_{ft}.In a simple relation, the ratio of $A_{ft}/A_{ref} = 0.7$ can be considered for the can and annular chambers and the ratio of $A_{ft}/A_{ref} = 0.65\sim0.67$ for the annular can combustion chamber [11]. Also, Eq. (11) provided by Bragg:

$$A_{ft} = 1.621 \times 10^{-2} \frac{\dot{m}_{fuel} T_3^{0.5}}{CPR} \left(\frac{P_3}{\Delta P}\right)^{0.5} \tag{11}$$

In addition, in the reference [2], in order to maximize the penetration ratio of the cooling fluid jet, Eq. (12) is proposed:

$$\left(\frac{A_{ft}}{A_{ref}}\right)_{opt} = 1 - \left(\frac{\dot{m}_{Annulus}}{\dot{m}_3}\right)^{2/3} \left(\frac{\Delta P_{3-4}}{q_{ref}}\right)^{-1/3} \tag{12}$$

Because Eq. (12) involves more parameters in the design, it is used in this study.

2-2-Diffuser and snout

After leaving the compressor, the air flow enters the diffuser of the combustion chamber, whose main function is to reduce the Mach (velocity) of the incoming flow and increase the static pressure. In the process of designing the diffuser, first the efficiency and then its dimensions are determined. The efficiency of the diffuser is a function of its divergence angle and is defined as follows:

$$\begin{aligned}\eta_{straight-wall} = {} & 1.1138 - 0.017701(2\theta) \\ & + 1.9925\times10^{-4}(2\theta)^2 \\ & - 9.3068\times10^{-7}(2\theta)^3 \\ & + 1.5722\times10^{-9}(2\theta)^4\end{aligned} \tag{13}$$

Then the flow weight function is calculated by Eq. (14).

$$wff = \sqrt{\frac{\gamma}{R}} M \left(1 + \frac{\gamma - 1}{2} M^2\right)^{-\frac{\gamma+1}{2(\gamma-1)}} \tag{14}$$

The flow weight function can be calculated at the inlet by knowing the Mach number at station 32. Also, the ratio of total to static pressure is obtained using Eq. (15). Although, the total pressure at station 32 is not known, but it is a function of the ideal pressure recovery coefficient and can be calculated using Eqs. (15) to (20) [12]:

$$\frac{P_{tot}}{P_{st}} = \left(1 + \frac{\gamma - 1}{2} M^2\right)^{\frac{\gamma}{\gamma-1}} \tag{15}$$

$$AR = \frac{A_{32}}{A_{31}} = \sqrt{\frac{1}{1 - C_{p,ideal}}} \tag{16}$$

$$C_p = \frac{P_{st32} - P_{st31}}{P_{dyn}} \quad (17)$$

$$\Delta P_{st} = C_p P_{dyn31} \quad (18)$$

$$P_{st32} = P_{st31} + \Delta P_{st} \quad (19)$$

$$P_{tot32} = P_{st32} \frac{P_{tot32}}{P_{st32}} \quad (20)$$

Then, the flow function is calculated again and if the new value matches the previous value, the solution is converged, otherwise, the solution method is repeated with the new assumption for the ideal recovery coefficient. The snout is placed between the diffuser and the initial area of the combustion chamber (before the swirler). The snout of the combustion chamber should be designed in such a way that the amount of air desired by the designer enters the annular section and the rest of the flow enters the combustion chamber through the holes of different areas. Therefore, the most important task of the snout is to divide the flow between the inlet core and the annular area of the combustion chamber. The cross-sectional area of the entrance snout is calculated from Eq. (21) [2].

$$\frac{A_{snout}}{A_{32}} = \frac{\dot{m}_{snout}}{\dot{m}_3} \frac{1}{C_{d.s}} \quad (21)$$

where $C_{d.s}$ is the snout coefficient, which in the ideal case (uniform output assumption) is considered to be equal to unity. Also, the mass flow rate of air passing through the snout $\dot{m}_{snout}$ is considered to be approximately equal to $\dot{m}_{pz}/2$. Eq. (22) is used to calculate the pressure drop in the snout section. [12]

$$\frac{\Delta P_{snout}}{q_{ref}} = 0.25 \frac{q_{snout}}{q_{ref}} = 0.25 \left(\frac{A_{ref}}{A_{32}}\right)^2 \quad (22)$$

2-3- Swirler

One of the components of the combustion chamber that has a direct effect on the flame structure, the level of pollutants and the overall efficiency of combustion is the swirler. The main task of the swirler is to convert a part of the axial velocity component into radial velocity [10]. Another task of the air swirler and primary holes is to create a return and vortex flow. Strong and stable return currents in the primary area cause flame stability and good fuel-air mixing, which makes the combustion chamber perform well in a wide range of flight conditions. The usual type of swirler includes a number of blades (usually 8 to 10) that are placed around the fuel injector at a specific angle [12]. The pressure drop in the combustion chamber includes the total pressure drop in the swirler, snout and diffuser. The swirler pressure drop is calculated from Eq. (23).

$$\frac{\Delta P_{SW}}{q_{ref}} = \frac{\Delta P_{3-4}}{q_{ref}} - \frac{\Delta P_{snout}}{q_{ref}} - \frac{\Delta P_{diff}}{q_{ref}} \quad (23)$$

The basis of the design of the dimensions of the impeller is based on the amount of pressure drop obtained in the thermodynamic analysis (zero dimension) of the gas turbine cycle. knight and walker proposed the following equation to express the relationship between pressure drop and the driving surface [13]:

$$\frac{\Delta P_{SW}}{q_{ref}} = K_{SW} \left[\left(\frac{A_{ref}}{A_{SW}}\right)^2 sec^2 \beta_{SW} - \left(\frac{A_{ref}}{A_{ft}}\right)^2 \left(\frac{\dot{m}_{SW}}{\dot{m}_3}\right)^2 \right] \quad (24)$$

where $\dot{m}_{SW}$ is the flow rate of the air entering the swirler, which is considered to be about 30-70% of the air in the primary entrance area. Also, based on experimental results, the amount of this air is considered to be 3-12% of the total incoming air (source 23).is also the air rotation K_{SW} coefficient, which is considered to be 1.3 in straight blades and 1.15 in curved blades. The swirler are usually made of

straight blade type and the air circulation angle(β_{SW})in them is considered to be about 45 to 70 degrees. After calculating the surface of the swirler, the outer radius of the swirler is calculated from Eq. (25).

$$r_{sw} = \sqrt{\frac{A_{SW}}{\pi} + r_{hub}^2} \tag{25}$$

Finally, the amount of rotation that the swirler applies to the flow is expressed by the swirler number, which is calculated by Eq. (26):

$$Swirl - number = \frac{2}{3}\tan\ \beta_{SW}\frac{(D_{hub}/D_{SW})^3}{(D_{hub}/D_{SW})^2} \tag{26}$$

2-4-Primary, secondary and dilution area

After injection, the fuel passes through three different areas. The first zone is the primary combustion zone, the task of this zone is to maintain the flame and also to provide enough time, temperature, and agitation so that the fuel sprayed in this zone completely combines with the incoming air, and the chemical energy hidden in it is converted into thermal energy. In other words, provide the conditions for a complete combustion. Fig. 3 shows the schematic of the rotating area of the combustion chamber.

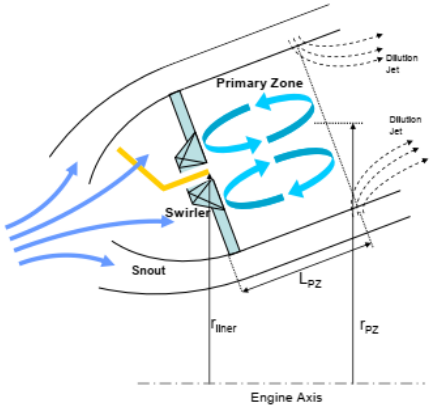

Fig. 3 Schematic of circulation area [12]

In order to place ignitors, the concept of magic circle is used. As shown in Figure 6, the magic circles are surrounded by the midline, the liner wall, and the dome wall of the liner. Also, this area is rich in fuel and air mixture, and the diameter of the magic circles is considered to be equal to half the diameter of the liner. The distance between the ignitors is calculated from Eq. (27) [14]:

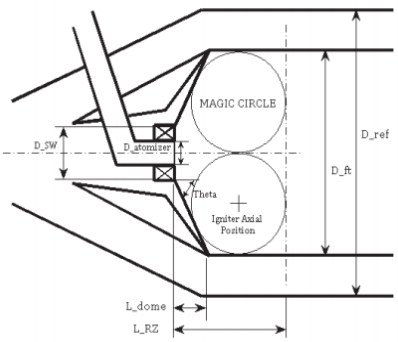

Fig. 4 Schematic of the rotating area and magic circles [15]

$$L_{ig} = \frac{D_{ft}}{4}\left[1 + cot\left(\frac{\pi - \theta_{dome}}{2}\right)\right] + L_{dome} - \frac{D_{ft}}{4} \tag{27}$$

where $\theta_{dome}$is the divergence angle of the diffuser, whose value is considered to be 60 degrees in conventional combustion chambers. Also, the length of the circulation area is equal to:

$$L_{RZ} = L_{igniter} + \frac{D_{ft}}{4} \tag{28}$$

Finally, knowing the swirler number and diameter of the swirler, the length of the primary area can be calculated with the following equation [2]:

$$L_{PZ} = D_{SW} \times Swirl - number \tag{29}$$

In the secondary area, with the addition of air currents, the combustion process is complete and we have the highest temperature (among the different areas of the combustion chamber), therefore, wall cooling in the middle area is one of the

most important issues in the design of the combustion chambers.

Then, in the dilution zone, the combustion flow is combined with the incoming air from the dilution zone and the output flow is regulated according to the turbine blades. Fig. 5 shows the distribution of air in different areas of the combustion chamber.

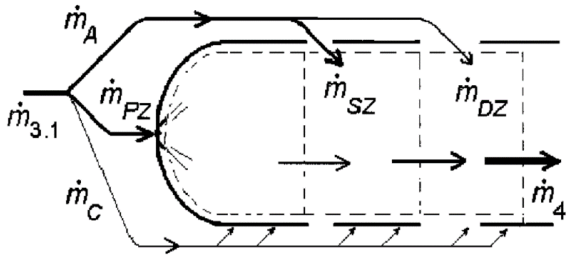

Fig. 5 Schematic of air distribution in different areas of the combustion chamber [2]

In this section, the details of calculating the holes of these two areas are briefly stated based on the ratio of the maximum penetration depth to the required jet diameter. The ratio of the maximum penetration depth to the jet diameter ($\frac{Y_{max}}{d_j}$) is defined by Eq. (30) [3]:

$$\frac{Y_{max}}{d_j} = 1.15J^{0.5}sin\theta \quad (30)$$

where θ is the penetration angle of the fluid jet and J is the ratio of the momentum flux of the fluid jet entering the gas (transverse flow), which is expressed as equation (31):

$$J = \frac{q_{jet}}{q_g} = \rho_{jet}U_{jet}^2\left(\rho_g U_g^2\right) \quad (31)$$

where q is the fluid momentum flux. According to the fact that the characteristics of the flow in the outlet section of the diffuser are known, the ratio of the maximum depth of penetration to the diameter of the fluid jet for the secondary area is calculated from equation (32).

$$\left(\frac{Y_{max}}{d_j}\right)_{SZ} = 1.15\sqrt{\frac{q_{jet}}{q_{32}}\left(\frac{q_{SZ}}{q_{32}}\right)^{-1}}\,sin\theta_{SZ} \quad (32)$$

Similar to the above equation is valid for the dilution zone. Then, by specifying the parameter $\frac{Y_{max}}{d_j}$ by the user (calculation input), the diameter of the dilution fluid jet is obtained by equation (33).

$$d_j = \left(\frac{Y_{max}}{D_{ft}}\right)\left(\frac{Y_{max}}{D_{ft}}\right)^1 D_{ft} \quad (33)$$

Considering that the effective area of the dilution flow is lower than the physical area, in terms of the flow coefficient c_d ,the effective area is defined by Eq. (34):

$$d_{orifice} = \frac{d_j}{\sqrt{c_d}} \quad (34)$$

The value of the flow coefficient parameter (c_d) depends on the flow conditions and the shape of the holes, and as a first approximation, its value can be considered constant [2], which is usually considered to be 0.6 to 0.65. The number of dilution holes is obtained by dividing the total input flow (secondary and dilution area) by the flow rate passing through a hole and is calculated by Eq. (35):

$$n_{orifices} = \frac{\dot{m}_{dilution}}{\dot{m}_{tot}}\frac{\dot{m}_{tot}}{\dot{m}_{jet}} = \frac{\dot{m}_{dilution}}{\dot{m}_{tot}}\frac{4A_{32}}{\pi\, d_j^2}\frac{V_{32}}{V_j} \quad (35)$$

Finally, Eq. (36) is used to determine the inlet fluid jet angle:

$$sin\theta = \sqrt{1 - \frac{q_{annulus}}{q_{jet}}} \quad (36)$$

The length of the secondary and dilution zones of the combustion chamber is

calculated based on the ratio of the length to the diameter of each zone.

Accurate calculation of each area requires accurate flow modeling, checking fuel-air mixing and heat transfer. Based on the information available in various references and reports, the ratio of the length to the diameter of the secondary and dilution areas is considered in the range of 0.5 to 1 [13]. In addition, the reference [10] suggested the length of the secondary region to be equal to the radius.

In different parts of the design algorithm, it is necessary to know the temperature of the fluid in different areas in order to calculate the dimensions and characteristics of the combustion chamber parts. It is assumed that the temperature in the initial zone should increase linearly from T_3 to T_{pz}. It is also assumed that the combustion is complete in the primary area and the combustion efficiency is about 99 in the secondary and dilution areas [16]. Therefore, the temperature in different areas is obtained from Eq. (37):

$$T_{out,zone} = T_3 + \eta_{zone}\Delta T_{zone} \quad (37)$$

To estimate the temperature increase ΔT_{zone}, curves are used that specify the temperature increase resulting from combustion as a function of inlet temperature, pressure and equivalence ratio [2]. It should be noted that in extracting the flow rate, pressure and, in general, a major part of the thermodynamic properties in different areas of the combustion chamber, ideal gas isentropic flow relations have been used.

3-Combustion chamber design and validation

In order to evaluate the presented design algorithm, the obtained results should be compared with the data of an existing engine. Due to the availability of geometric and thermodynamic data of the CFM56-7B27 engine, the data of the combustion chamber of this engine have been used to validate the design. Fig. 6 shows the two-dimensional design of the mentioned combustion chamber. The cyclic parameters of this combustion chamber in different flight conditions are presented in Table 1 and the necessary input parameters for use in the design algorithm are presented in Table 2 [13].

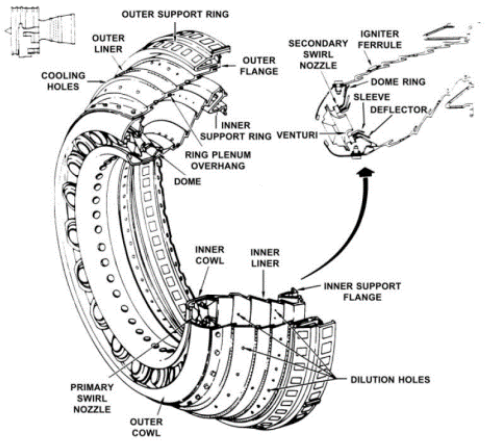

Fig. 6 Schematic of the combustion chamber of CFM56-7b27 engine [17]

According to the presented design algorithm, in the first step, the reference diameter and the liner diameter of the combustion chamber are estimated. Using the data of Tables 1 and 2, as input to the problem, the reference diameter was calculated with different methods, and the results obtained are shown in Table 3.

Table 1: Cyclic parameters of the combustion chamber in different operating conditions[12]

Cond.	Total inlet temperature (K)	Total inlet pressure (k Pa)	Fuel flow rate (kg/sec)	air flow rate (kg/sec)	Total equivalence ratio
Take-off	800	2900	1.276	44.52	0.42
Climb	764	2477	1.040	39.10	0.39
Approach	613	1132	0.349	20.87	0.245
Ground idle	505	559	0.119	12.12	0.144

Table 2: Set of necessary input parameters to determine the dimensions of the combustion chamber of the CFM56-7B27 engine [12]

paremeter	value
Pressure factor	45
Pressure loss ratio	0.05
equivalence ratio in on-design condition	1.05
equivalence ratio in on-design condition	0.8
Mach number at Outer annuli	0.015
Mach number at the end of PZ	0.05
Inlet mean radius (compressor exit)	275.8 mm
Exit mean radius (turbine entrance)	344.4 mm
Number of injectors	20
Divergence half angle of diffuser	1.2
Diffuser inlet height	19.6 mm
Maximum area ratio of straight wall diffuser (sweet-spot)	1.25
Diffuser inlet Mach number (M31)	0.2
Diffuser exit Mach number (M32)	0.04
Combustor exit Mach number (M40)	0.075
Fuel inlet temperature	309 K
Maximum allowable liner temperature	1139 K
Cooling mechanism factor	0.29
Swirl angle	61.5 degree
Swirler discharge parameter(K_{sw})	1.3
Ratio of atomizer diameter to reference diameter	0.1
Burner dome angle	60 degree
Dilution holes discharge coefficient (c_d)	0.6
Penetration depth to flame tube diameter at DZ	0.41
Penetration depth to flame tube diameter at SZ	0.46

Table 3: Reference diameter values calculated from the conceptual design (all units are in meters)

Cond.	AeroDyn	Chemical	Odgers	Comb. Loading
Take-off	0.103	0.019	0.188	0.098
Climb	0.104	0.022	0.200	0.095
Approach	0.109	0.043	0.263	0.073
Ground idle	0.116	0.077	0.322	0.052

In the calculated results for the reference diameter in different working conditions, different values have been obtained, but the design conditions are more important. the reference diameter should be large enough to meet the aerodynamic and combustion requirements. In the CFM56 engine, the reference diameter is 0.126 m and the liner diameter is 0.0861 m. Also, the ratio of the cross-sectional area of the liner to the cross-sectional area of the combustion chamber is about 0.68, which

is in acceptable agreement with the equations proposed in the references. Using the presented algorithm, the geometric and thermodynamic characteristics of the desired combustion chamber are calculated, Table 4 shows the geometrical parameters and Table 5 shows the thermodynamic characteristics of the combustion chamber.

Table 4: Geometric values calculated from the algorithm compared to the actual values of the combustion chamber (all units are in meters)

Geometrical parameters	Calculated data	Refrence data	Error percentage
Diffuser length	0.102	0.0795	22
PZ length	0.054	0.0531	1.6
SZ length	0.056	0.0597	6.6
DZ length	0.074	0.0648	12.4
Dome length	0.0144	0.014	2.7
Atomizer diameter	0.0126	0.013	3.1
Swirler hub radius	0.0189	0.0145	23
Swirler tip radius	0.03	0.023	23
SZ orifices number	72	80	11
DZ orifices number	100	120	20

Table 5: Thermodynamic results calculated by the design algorithm (all units are in SI)

mode	Diffuser outlet				primary zone outlet			
	Temp.	velocity	Mach number	pressure	Temp.	velocity	Mach number	pressure
1	800	20.14	0.04	2799	1753.4	34.04	0.042	2796
2	763.9	19.77	0.04	2390	1712.4	31.81	0.039	2382
3	612.9	18.17	0.04	1090	1501.1	20.92	0.027	1065
4	504.9	16.82	0.04	537	1327.4	13.31	0.017	505

mode	Secondary Zone outlet				Combustion chamber outlet			
	Temp.	velocity	Mach number	pressure	Temp.	velocity	Mach number	pressure
1	1748.5	36.16	0.050	2795	1692.6	42.43	0.060	2794
2	1706.9	33.71	0.047	2381	1632.9	40.02	0.057	2380
3	1492.9	21.88	0.032	1065	1264.7	28.58	0.043	1065
4	1317.9	13.80	0.021	505	951.6	20.98	0.035	505

The design was compiled based on various equations and recommendations from available sources, and the results obtained according to the purpose of the research, which is in the conceptual design stage, have an acceptable error compared to the original values. By using this design algorithm, it will be possible to design combustion chamber components and produce two-dimensional geometry.

4-Afterburner design

In this section, the conceptual design of the afterburner is discussed. Since there is no specific reference in the afterburner design that directly expresses the governing equations, according to the articles and studies conducted in this field, it has been tried to extract the design relations.

In addition, some information is also obtained from the reverse engineering method.

4-1-Design of afterburner components

Similar to the combustion chamber, the first step in afterburner design is to calculate the diameter. Considering that the input conditions are known, the afterburner area is calculated according to Eqs. (38) and (39).

$$A_{ab} = \frac{\dot{m}_{in}}{V_{in}\rho_{in}} \tag{38}$$

$$R_{ab} = \sqrt{Aab/\pi} \tag{39}$$

It should be noted that the obtained value is the minimum diameter required for the design of the afterburner and higher values decrease the speed and thus improve the combustion stability. Fig. 7 shows the main parameters used in afterburner design at the conceptual design level.

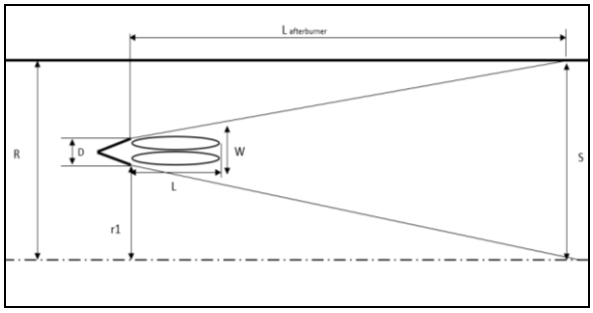

Fig. 7 Main parameters in afterburner design

One of the most important input parameters is the equivalence ratio. By determining the type of fuel, in order to reach the expected temperature, the equivalence ratio is calculated according to Eq. (40). It should be considered that in the afterburner, unlike the combustion chamber, the equivalence ratio is considered dilute, except for the case where we want to reach a high temperature at the outlet .

$$\varphi = \left(\frac{q}{LHV}\right)\left(\frac{\left(\frac{A}{F}\right)_s}{\eta}\right) \tag{40}$$

Considering that in the conceptual design phase, the fuel is considered as a mixture of fuel and air, there is no need to design a fuel injector. In the afterburner, a flame holder is used to maintain the flame. In turbofans and turbojets, generally flame holders or V-gutters are used, which are placed inside the afterburner as annular or radial elements. When the flow of fuel and air mixture passes through the flame holders, a large rotating area is created behind the flame holder, which provides enough time for the combustion reaction, and as the flame spreads from this area, the combustion spreads throughout the afterburner. The use of several V-Gutter rings reduces the length of the afterburner, but on the other hand, the pressure drop increases and the relationships governing it become more complicated. In this work, because we do not have a length limit and in order to prevent pressure drop, a single-ring V-Gutter has been used. Fig. 8 shows the schematic of a V-Gutter flame keeper.

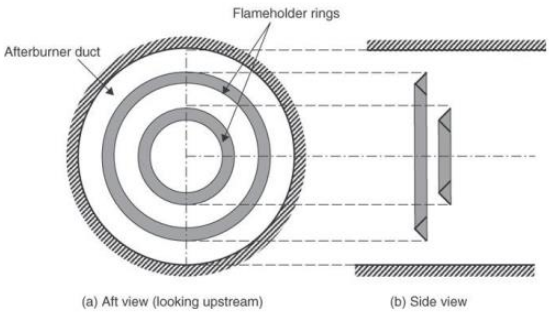

Fig. 8 Schematic of a V-Gutter flame keeper [18]

One of the main design requirements of most combustion systems is to keep the flame burning under a wide range of operating conditions. According to Eq. (41) Lefebvre and Ballal [19] have predicted the range of flame extinction by

considering the parameters of speed, temperature, pressure, velocity, turbulence, equivalence ratio and blockage coefficient:

$$\emptyset_{W.E} = \left(\frac{2.25(1+0.4U[1+0.1T_u}{P^{0.25}T_0\exp(T_0/150)D(1-B)}\right)^{0.16} \quad (41)$$

In Eq. (53) $\emptyset_{W.E}$ is the equivalence ratio of the flame extinction limit in the state of dilute mixture, B is the blocking ratio and D is the afterburner diameter, and this relation expresses the flame extinction limit.

The above relation for flame holder width, as the most important geometric size in flame holder design, has been rewritten and given as Eq. (42).

$$D = \frac{1.35U + 2.25}{\varphi^{6.25}T(B-1)(Pe^{\frac{2T}{75}})^{0.25}} \quad (42)$$

In Eq. (43), the minimum width of the flame holder is directly calculated, and in the design process, the value of this parameter should be considered higher than the obtained value for the stability of the flame.

Also, in this equation, the effect of turbulence is omitted due to its very small effect. Another parameter of the flame holder design is the angle of the V-gutters. Reference [2] has suggested an angle of 30 degrees for the purpose of optimization, which is considered the same value in the present work.

The placement position of the V-gutter has a great effect on the length of the afterburner. Eq. (43) is provided to calculate the placement position of the V-gutter with respect to the afterburner axis r_1.

$$r_1 = \frac{(BR^2) - D^2}{2D} \quad (43)$$

In order to achieve the shortest desired afterburner, r_1 should be equal to half the radius of the afterburner. Therefore, the dependent parameters should be considered in such a way that this requirement is met. The afterburner design algorithm is shown in figure (9).

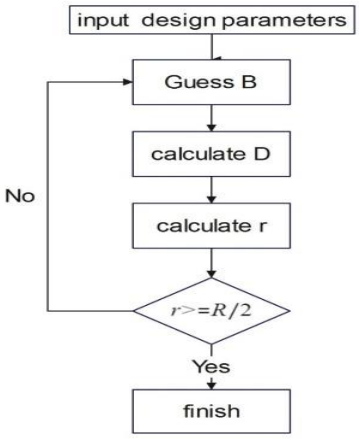

Fig. 9 Algorithm for calculating the radial distance V-Gutter from the afterburner axis

One of the other parameters in the design of afterburners is the length of the afterburner. The length of the afterburner is a function of the arrangement of the flame holders and the flame spread angle, the flame spread angle is independent of the type of fuel, the inlet flow rate and the equivalence ratio [20]. The flame spread angle is dependent on the amount of flow turbulence and the temperature of the inlet stream, since exact relations for calculating the flame spread angle were not available, with the help of reverse engineering of some existing operational afterburners, the range of the flame spread angle was rewritten. It should be noted that different sources were used to derive this angle, of which only one example is shown in Fig. 10. Finally, the study of different cases showed that in practice this angle is considered between 2 and 4 degrees

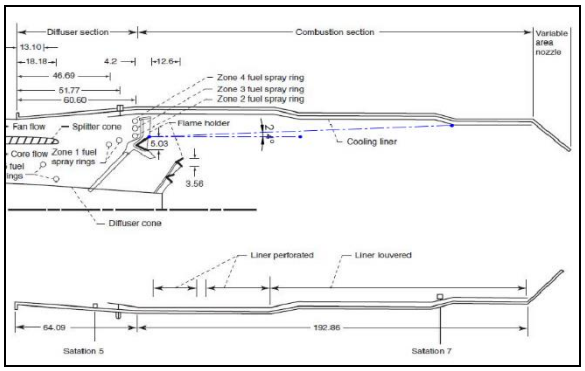

Fig. 10 The flame spread angle of TF-30 afterburner design [20]

With the flame spreading angle, finally the length of the afterburner is calculated with simple trigonometric relationships with the help of Eq. (44).

$$L_{AB} = \cot\alpha \times \frac{R}{2} \tag{44}$$

where R is the afterburning radius and α is the flame spreading angle.

4-2- Calculation of afterburner output parameters

As stated at the beginning of the design, the outlet temperature in the afterburner design is one of the input parameters that is determined according to the equivalence ratio, and therefore the outlet temperature does not need to be calculated. The next parameters are the output Mach and the pressure drop ratio calculated in the Reheat Mode and Dry Mode. Eqs. (45) to (48) have been used to calculate the flow output Mach, pressure drop ratio and drag coefficient of the element in the Dry Mode, respectively. [3]

$$M_e^2 = \frac{2(\gamma_e - 1) - \gamma_e A^2}{(\gamma_e - 1)(A^2 - 2)} + \frac{\sqrt{(\gamma_e A^2 - 2\gamma_e + 2)^2 + 2(\gamma_e - 1)^2(A^2 - 2)}}{(\gamma_e - 1)(A^2 - 2)} \tag{45}$$

$$A = \left(\frac{1 + \gamma_i M_i^2\left(1 - \frac{C_D}{2}\right)}{\gamma_i M_i}\right)\sqrt{\frac{\gamma_i - 1}{1 + \frac{\gamma_i - 1}{2}M_i^2}} \tag{46}$$

$$\frac{P_{te}}{P_{ti}} = \frac{P_e}{P_i}\frac{\left(1 + \frac{\gamma_e - 1}{2}M_e^2\right)^{\frac{\gamma_e}{\gamma_e - 1}}}{\left(1 + \frac{\gamma_i - 1}{2}M_i^2\right)^{\frac{\gamma_i}{\gamma_i - 1}}} = \frac{1 + \gamma_i M_i^2\left(1 - \frac{C_D}{2}\right)}{1 + \gamma_e M_e^2}\frac{\left(1 + \frac{\gamma_e - 1}{2}M_e^2\right)^{\frac{\gamma_e}{\gamma_e - 1}}}{\left(1 + \frac{\gamma_i - 1}{2}M_i^2\right)^{\frac{\gamma_i}{\gamma_i - 1}}} \tag{47}$$

$$C_B = B.C_{D\ bluff-body} \tag{48}$$

In Eq. (48), $C_{D\ bluff-body}$ is the equivalent drag coefficient and its value is calculated experimentally, and in reference [4], the value of 1 is suggested for V-Gutter's flame holder. For the Reheat Mode, according to reference [3], for the outlet Mach, the pressure drop ratio and the drag coefficient of the element are proposed according to the Eqs. (49) to (52).

$$M_e^2 = \frac{2(\gamma_e - 1) - \gamma_e A^2}{(\gamma_e - 1)(A^2 - 2)} + \frac{\sqrt{(\gamma_e A^2 - 2\gamma_e + 2)^2 + 2(\gamma_e - 1)^2(A^2 - 2)}}{(\gamma_e - 1)(A^2 - 2)} \tag{49}$$

$$A = \left(\frac{1 + \gamma_i M_i^2\left(1 - \frac{C_D}{2}\right)}{\gamma_i M_i}\right) \times \sqrt{\frac{\gamma_i - 1}{1 + \frac{\gamma_i - 1}{2}M_i^2}\left(\frac{1}{\frac{c_{pe}T_{te}}{c_{pi}T_{ti}}}\right)} \tag{50}$$

$$\frac{P_{te}}{P_{ti}} = \frac{P_e}{P_i}\frac{\left(1 + \frac{\gamma_e - 1}{2}M_e^2\right)^{\frac{\gamma_e}{\gamma_e - 1}}}{\left(1 + \frac{\gamma_i - 1}{2}M_i^2\right)^{\frac{\gamma_i}{\gamma_i - 1}}} = \frac{1 + \gamma_i M_i^2\left(1 - \frac{C_D}{2}\right)}{1 + \gamma_e M_e^2}\frac{\left(1 + \frac{\gamma_e - 1}{2}M_e^2\right)^{\frac{\gamma_e}{\gamma_e - 1}}}{\left(1 + \frac{\gamma_i - 1}{2}M_i^2\right)^{\frac{\gamma_i}{\gamma_i - 1}}} \tag{51}$$

$$C_B = B.C_{D\ bluff-body} \tag{52}$$

4-3- Afterburner design results

Considering that the aircraft is subjected to different input conditions in different flight conditions and also the performance parameters such as temperature and equivalence ratio are not uniformly

distributed across the width of the engine, the design is considered conservative and for the worst performance conditions. Therefore, the inlet conditions to the afterburner are considered according to Table 6.

Table 6: Afterburner design input parameters

Inlet parameters	value
air flow rate	40 kh/sec
Inlet speed to afterburner	90 m/s
Inlet air temperature	500 k
inlet pressure	500 kpa
V-Gutter angle	30 degree
Angle of flame spread	4 degree

The results obtained by the presented design algorithm are shown in Table 7. By using the obtained algorithm, in addition to calculating the dimensions of the flame holder, it is also possible to calculate the characteristics of the output flow.

Table 7: Afterburner geometric and functional parameters

Parameter	value
Design equivalence ratio	0.5
V-Gutter width	0.03 m
The radial distance of the V-Gutter from the afterburner axis	0.2 m
afterburner length	2.8 m
Element drag coefficient	0.2
Output pressure drop ratio in off afterburner mode	0.98
Output pressure drop ratio in afterburner mode	0.92
Afterburner output Mach number in off afterburner mode	0.23
Output Mach number in afterburner mode	0.41

5- Conclusion

1- The results of the conceptual design of the combustion chamber were in good agreement with the real model and more details were checked than the existing designs, hence the cost and time of simulation and laboratory testing and finally reaching the final design are reduced.

2- In addition to the possibility of parametric study of the combustion chamber and afterburner, the presented algorithm also provides the possibility of their optimization, so it can be done with very little cost and time compared to simulation and laboratory methods.

3- The proposed design can supply the inlet flow to the nozzle without using a turbine, therefore, in addition to innovation in similar cases (nozzle test air supply equipment), it can be done with a lower financial cost.

4- Combustion chamber design requires multiple laboratory tests and the final design is obtained through an iterative process. Therefore, in the conceptual design phase, the more accurate and detailed the design is, the shorter the design process will be. Considering that the present design has examined many parameters, it can reduce the construction time with the better and deeper knowledge it creates.

5- In the afterburner design, in addition to analytical relations, reverse engineering is also used, which makes the design closer to the real designs.

6- One of the most important challenges for afterburner designers is flame stability. In the present work, a relation based on experience was used for the design of the flame holder, which, in addition to being formulated based on the flame extinction limit, many parameters are also effective in it.

References

[1] W. Dodds and D. Bahr. (1990). Combustion system design. *Design of modern gas turbine combustors*, pp.343-476.

[2] J. D. Mattingly. (2002). *Aircraft engine design*: AIAA.

[3] A. H. Lefebvre. (2010). *Gas turbine combustion*. CRC Press.

[4] M. R. J. Charest. (2006). Design methodology for a lean premixed prevaporized can combustor. MS Thesis, Library and Archives Canada,Carleton University, Department of Mechanical and Aerospace Engineering.

[5] P. J. Stuttaford and P. A. Rubini. (1996). Preliminary gas turbine combustor design using a network approach. *In ASME International Gas Turbine and Aeroengine Congress and, Exhibition*.

[6] P. J. Stuttaford and P. A. Rubini**.** (1996) Preliminary gas turbine combustor design using a network approach. *in ASME International Gas Turbine and Aeroengine Congress and, Exhibition*.

[7] M. J. Wankhede. (2012). Multi-fidelity strategies for lean burn combustor design. PhD Thesis, University of Southampton.

[8] Jai-Houng Leu. (2010). Design and simulation validation of LHV fuel combustor . *Journal of Information and Optimization Sciences*, 31:6,1321-1336.

[9] Yize Liu, Xiaoxiao Sun, Vishal Sethi, Yi-Guang Li, Devaiah Nalianda, David Abbott, Pierre Gauthier,Bairong Xiao and Lu Wang. (2021). Development and application of a preliminary design methodology for modern low emissions aero combustors. *Journal of power and energy*. Vol. 235(4) 783-806.

[10] J. W. Sawyer. (1966). Gas Turbine Engineering Handbook: Editor. *John W. Sawyer, vol.* 1*, Gas Turbine Publications*.

[11] P. P. Walsh and P. Fletcher. (2004). Gas turbine performance**.** *John Wiley & Sons.*

[12] R. Rezvani. (2010). A Conceptual Methodology for the Prediction of Engine Emissions. PhD Thesis, Georgia Tech. University.

[13] H. Knight and R. Walker. (1953). The component pressure losses in combustion chambers. *Gt. Brit. National Gas Turbine Establishment, Farnborough, Hants, England*.

[14] M. R. J. Charest. (2006). Design methodology for a lean premixed prevaporized can combustor. MSThesis, Library and Archives Canada Bibliothèque et Archives Canada, Carleton University, Department of Mechanical and Aerospace Engineering.

[15] A. Costa Conrado, P. T. Lacava, A. C. P. Filaho, M. D. S. Sanches. (2004). Basic design principles for gas turbine combustor. *Proceedings of the 10o Brazilian Congress of Thermal Sciences and Engineering*.

[16] J. J. Gouws. (2008). Combining a one-dimensional empirical and network solver with computational fluid dynamics to investigate possible modifications to a commercial gas turbine combustor. MS Thesis, University of Pretoria.

[17] K. A. das Neves. (2018). Combustion analysis on a CFM56 engine. Master's Degree in Aeronautic engineering, Beira Interior University.

[18] S.Farokhi. Aircraft Propulsion. second Edition, Wiley.

[19] A.Lefebvre-D.Ballal. (1979). Weak Extinction Limits of Turbulent Flowing Mixtures**.** *Journal of Engineering for Power*.

[20] E. zukoski. (1985). Aerothermodynamics of Aircraft Engine Components. AIAA.